Hindawi
BioMed Research International
Volume 2022, Article ID 3605054, 7 pages
https://doi.org/10.1155/2022/3605054

Research Article

Enhanced Thermal Stability and Synergistic Effects of Magnesium and Iron Borate Composites against Pathogenic Bacteria

Pervaiz Ahmad,[1] **Mayeen Uddin Khandaker**,[2,3] **Abdulhameed Khan**,[4] **Fida Rehman**,[5] **Salah Ud Din**,[6] **Hazrat Ali**,[7] **Muhammad Imtiaz Khan**,[7] **Nawshad Muhammad**,[8] **Nasar Ahmed**,[1] **Zahoor Ullah**,[9] **Ghulamullah Khan**,[10] **Sirajul Haq**,[6] **Talha Bin Emran**,[11,12] **Rohit Sharma**,[13] **and I. M. Ashraf**[14,15]

[1]*Department of Physics, University of Azad Jammu and Kashmir, 13100 Muzaffarabad, Pakistan*
[2]*Center for Applied Physics and Radiation Technologies, School of Engineering and Technology, Sunway University, Bandar Sunway, 47500 Selangor, Malaysia*
[3]*Department of General Educational Development, Faculty of Science and Information Technology, Daffodil International University, DIU Rd, Dhaka 1341, Bangladesh*
[4]*Department of Biotechnology, University of Azad Jammu and Kashmir, 13100 Muzaffarabad, Pakistan*
[5]*Department of Physics, Khushal Khan Khattak University, 27200 Karak, Khyber Pakhtunkhwa, Pakistan*
[6]*Department of Chemistry, University of Azad Jammu and Kashmir, 13100 Muzaffarabad, Pakistan*
[7]*Department of Physics, Abbottabad University of Science and Technology, Havelian, Khyber Pakhtunkhwa, Pakistan*
[8]*Department of Dental Materials, Institute of Basic Medical Sciences, Khyber Medical University Peshawar, Khyber Pakhtunkhwa 25100, Pakistan*
[9]*Department of Chemistry, Takatu Campus, Balochistan University of IT, Engineering and Management Sciences (BUITEMS), Quetta 87100, Pakistan*
[10]*Department of Engineering and Architecture, Takatu Campus, Balochistan University of IT, Engineering and Management Sciences (BUITEMS), Quetta 87100, Pakistan*
[11]*Department of Pharmacy, BGC Trust University Bangladesh, Chittagong 4381, Bangladesh*
[12]*Department of Pharmacy, Faculty of Allied Health Sciences, Daffodil International University, Dhaka 1207, Bangladesh*
[13]*Department of Rasa Shastra and Bhaishajya Kalpana, Faculty of Ayurveda, Institute of Medical Sciences, Banaras Hindu University, Varanasi, 221005 Uttar Pradesh, India*
[14]*Physics Department, Faculty of Science, King Khalid University, Abha 9004, Saudi Arabia*
[15]*Physics Department, Faculty of Science, Aswan University, Aswan, Egypt*

Correspondence should be addressed to Pervaiz Ahmad; pervaiz_pas@yahoo.com
and Mayeen Uddin Khandaker; mayeenk@diu.edu.bd

Received 6 August 2022; Revised 18 September 2022; Accepted 27 September 2022; Published 14 November 2022

Academic Editor: Mahmoud Kandeel

A simple process based on the dual roles of both magnesium oxide (MgO) and iron oxide (FeO) with boron (B) as precursors and catalysts has been developed for the synthesis of borate composites of magnesium and iron ($Mg_2B_2O_5$-Fe_3BO_6) at 1200°C. The as-synthesized composites can be a single material with the improved and collective properties of both iron borates (Fe_3BO_6) and magnesium borates ($Mg_2B_2O_5$). At higher temperatures, the synthesized $Mg_2B_2O_5$-Fe_3BO_6 composite is found thermally more stable than the single borates of both magnesium and iron. Similarly, the synthesized composites are found to prevent the growth of both gram-positive (*Staphylococcus aureus*) and gram-negative (*Escherichia coli*) pathogenic bacteria on all the tested concentrations. Moreover, the inhibitory effect of the synthesized composite increases with an increase in concentration and is more pronounced against *S. aureus* as compared to *E. coli*.

1. Introduction

Commercially available boron-based compounds, especially borates, are very important due to their ultimate uses in a wide range of potential applications [1]. Magnesium borates (like $Mg_2B_2O_5$) and iron (Fe-III) borates (like Fe_3BO_6) are the two well-known borates in the borate family.

$Mg_2B_2O_5$ is a magnesium borate with excellent thermal stability. Being thermodynamically stable, it has great potential to be used in making devices for working in a higher temperature environment. Besides, $Mg_2B_2O_5$ has a great tensile strength (mechanical properties) and excellent thermoluminescent properties. It is a remarkable functional material [2], with excellent anticorrosion and antiwear behavior [3, 4]. $Mg_2B_2O_5$ has potential applications as catalysts (for hydrocarbon conversion) and as a wide band gap semiconductor. It is used as reinforcing elements for aluminum/magnesium alloy matrix and plastics. Magnesium borates have the characteristics of thermoluminescent materials; therefore, $Mg_2B_2O_5$ can be used in fluorescent discharge lamps and X-ray screens [5].

Like $Mg_2B_2O_5$, Fe_3BO_6 (called Fe-III borates) is also a well-known borate in the iron borate family [6]. The main uses of these materials are found as electrodes in lithium-ion batteries. These electrodes (made from Fe_3BO_6) are used as power sources in electric and hybrid vehicles. Similarly, Fe_3BO_6 is used in biological probes and gas sensors [7]. Besides, Fe_3BO_6 can be used to work as a weak ferromagnetic switch due to its unique spin reorientation [7].

Borate compounds have excellent biocompatibility and can, therefore, be used for a series of potential applications in different biomedical fields. Likewise, borates are environmentally friendly and have a lot of potential applications in modern technology [7, 8]. The combination of borates with different bioactive materials can offer great potential in their usage in biomedical applications to avert infections. Besides borates, boron-doped silver-copper alloy nanoparticles are also very effective in eradicating *S. aureus* infection from bone cells [9].

Both of these borates ($Mg_2B_2O_5$ and Fe_3BO_6) from magnesium and iron families have excellent properties for different applications in the advanced technologies. As a result, different types of structures (both in bulk and nano) of the above borates have been reported by different researchers in the literature. These included nanowires, nanorods, and whiskers. Most of the nanostructures of $Mg_2B_2O_5$ have been obtained via chemical vapor deposition (CVD) [10], solvothermal [11], catalyst-free method [12], and solid-state synthesis, respectively [5]. However, most of the reported techniques for $Mg_2B_2O_5$ synthesis were found to base on multisteps consisting of gas or liquid phase processes. At the same time, the yield was low and hence an economical method has been sought for the production of $Mg_2B_2O_5$ [5]. Likewise, different nanostructures of Fe_3BO_6 have also been reported by solid-state reaction [13], solution-phase reaction [14, 15], hydrothermal method, etc. [16]. Again, the overall reported techniques are not only difficult to follow, time-consuming, or lengthy but also reported to have some of the as-used precursors or their compounds in the final product as impurities.

Regardless of the pros and cons of the reported techniques, $Mg_2B_2O_5$ and Fe_3BO_6 are synthesized in various sizes, shapes, or morphologies. Each of the borate synthesis techniques either talks about $Mg_2B_2O_5$ (or other magnesium borates) or Fe_3BO_6 (or other iron borates) in both bulk and nano for their potential applications in modern technology. However, none of the techniques so far have ever been developed to work on the synthesis of both the products as a composite. At the same time, if a technique is developed for the synthesis of borate composites ($Mg_2B_2O_5$ and Fe_3BO_6), one has to make sure not only about the quality but also about the quantity of the final product. Quality and quantity are the two main parameters that need to be judged for any synthesized product to be used for its potential application. Along with the quality and quantity, the size and crystallinity of the materials also significantly change the properties to a great extent [17].

Here, we report a unique and facile technique for the synthesis of highly crystalline $Mg_2B_2O_5$ and Fe_3BO_6 composites from carbon-free precursors in a growth duration of one hour at 1200°C in a graphite crucible. The as-synthesized crystalline composites of $Mg_2B_2O_5$ and Fe_3BO_6 are sought to have excellent properties for their potential applications in the field of biomedical particularly in the inhibition of pathogenic bacteria. Therefore, these composites have successfully been used via the agar well diffusion method to test their antibacterial activity against both gram-positive and gram-negative pathogenic bacteria.

2. Experimental Details

2.1. Synthesis Procedure. Highly crystalline $Mg_2B_2O_5$-Fe_3BO_6 composites are synthesized from a powder mixture of boron (B), iron oxide (FeO), and magnesium oxide (MgO). All the precursors were of analytical grade with a high purity of 99.999%, purchased from the Sigma-Aldrich, USA. At first, one gram powder of boron is taken in a graphite crucible. Afterward, 0.5 gram Mg powder is added to the boron powder in the crucible and homogeneously stirred for a few minutes. Consequently, 0.5 gram of FeO is also added to the crucible and properly mixed with (the mixture of) boron and MgO. The top of the crucible (open-side) is carefully covered by its graphite cap. The covered (closed) crucible (with precursors) is then placed inside the furnace for heating up to 1200°C in the argon atmosphere (where it has been kept for one hour). Afterward, the set-up is slowly brought to room temperature. The synthesized sample is carefully collected from the furnace at room temperature and characterized by different characterization apparatuses to observe its composition, phase, structure, and morphology.

2.2. Antibacterial Assay. The agar well diffusion method was used to test the antibacterial activity of $Mg_2B_2O_5$-Fe_3BO_6 composites, against both gram-positive and gram-negative pathogenic bacteria [18]. The overnight grown culture of *E. coli* and *S. aureus* was used to assess the antibacterial activity of $Mg_2B_2O_5$-Fe_3BO_6 composites. Bacterial suspensions of *E. coli* and *S. aureus* of 1.5×10^8 CFU/ml

concentration were inoculated on Muller-Hinton agar plates and spread uniformly via a sterile cotton swab. The same bacterial concentrations and culture medium were used for all experiments. Wells were made via a sterile polystyrene tip (4 mm). Different concentrations of $Mg_2B_2O_5$-Fe_3BO_6 (20, 40, 60, 80, and 100 mg/ml) were freshly dissolved in DMSO (dimethyl sulfoxide) and added to separate wells. The plates were incubated for 24 hours at 37°C. The antibacterial activity was determined by measuring the diameter of the zone of inhibition (ZOI) produced by $Mg_2B_2O_5$-Fe_3BO_6 around each well. Antibiotic clindamycin phosphate was used as a positive control to compare the antibacterial activity of $Mg_2B_2O_5$-Fe_3BO_6.

3. Results and Discussion

The mixture of boron, FeO, and MgO was found to be an effective precursor in the synthesis of high yield boron nitride nanotubes [19–21]. After being through the initial stages with the catalytic activity of Mg and Fe with the boron, the mixture finally reacts with ammonia at higher temperatures and results in the synthesis of BNNTs. The current work is somehow similar to the previous work regarding the choice of precursors and different with respect to the use of reactive gases and experimental setup. Unlike previous, the precursors are cap-closed in the crucible. To avoid any possible contamination (as the cap of the crucible is not sealed closed) from the surrounding, argon flow is maintained throughout the whole process. No reactive gas is used. Simply, the reactants are heated up to 1200°C and kept for one hour. The following chemical reaction occurs at higher temperatures:

$$3B + 2MgO + 3FeO + 3O_2 \longrightarrow Fe_3BO_6 + Mg_2B_2O_5 \quad (1)$$

As a result of these reactions, highly crystalline composites of Fe_3BO_6 and $Mg_2B_2O_5$ are formed at a higher temperature of 1200°C. Here, it is worth mentioning that boron has a high melting point. In the amorphous form, it melts at around 2300°C, whereas in the form of α-rhombohedral crystals, it melts at 2180°C [22]. Thus, based on the desires for the final product and choice of the reaction, some suitable catalysts are used to not only melt boron at an affordable temperature but also easily recovered it if not needed in the final product. Luckily, MgO and FeO have already been found to soften boron at relatively low temperatures [23]. Beside, Mg, Fe, and O are also needed as elemental contents in the required composites. Therefore, these two metal oxides are chosen to work both, initially as catalysts (soften boron to melt at a relatively lower temperature) and finally as reactants with boron to form $Mg_2B_2O_5$-Fe_3BO_6 composites.

The synthesized $Mg_2B_2O_5$-Fe_3BO_6 composites are characterized by an X-ray diffractometer (XRD) to check their crystalline nature, composition, and phase. The resulted XRD pattern is displayed in Figure 1. There are several peaks in the displayed XRD pattern, which points toward the highly crystalline nature of the synthesized composites.

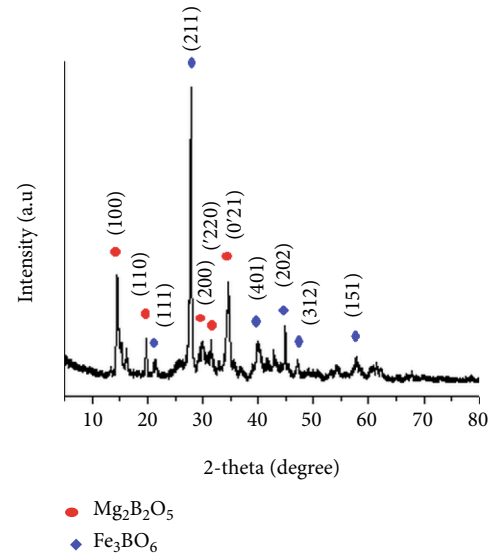

Figure 1: XRD pattern of the as-synthesized $Mg_2B_2O_5$-Fe_3BO_6 composites.

The peak position corresponds to the formation of different compounds in the sample. There are several peaks in the spectrum (at different 2-theta values) tagged in blue. These peaks according to the available literature correspond to (111), (211), (401), (202), (312), and (151) planes in Fe_3BO_6 [15, 24]. Similarly, there are several more peaks in the XRD pattern tagged in red. These red-tagged peaks in the XRD pattern stand for the planes (100), (110), (200), ($'220$), and ($0'21$) in the synthesized $Mg_2B_2O_5$ sample according to the literature [3, 12, 25]. The existence of both the compounds ($Mg_2B_2O_5$ and Fe_3BO_6) in the sample pointed toward the formation of $Mg_2B_2O_5$-Fe_3BO_6 composites. The formation of these composites is confirmed in scanning electron microscopy (SEM). SEM was needed not only to check the morphology or structure of the synthesized composites but also to observe whether both the compounds are parts of the same crystals or not.

Figure 2 shows the SEM micrograph of the synthesized $Mg_2B_2O_5$-Fe_3BO_6 composites. The micrograph shows randomly aligned fine crystals of $Mg_2B_2O_5$-Fe_3BO_6 composites in different sizes and morphologies. None of the crystals looks identical in shape. According to the given scale in the micrograph, the sample contained crystals with a diameter in the range of 0.5–4 μm. Some of the crystals are sharp and seem like randomly broken pieces of ice. Agglomerated clots of crystals can also be seen in the sample near the left-hand bottom corner of the micrograph. A few round fiber-like crystals are also found in the middle of the micrograph indicated in a white circle. The magnified view of these crystals is shown in the inset in the upper right-hand corner. The magnified view clarifies the single body structure of the composites made from $Mg_2B_2O_5$ and Fe_3BO_6. Some small agglomerated structures are also indicated in the sample via a white rectangle. These structures are magnified and shown as an inset on

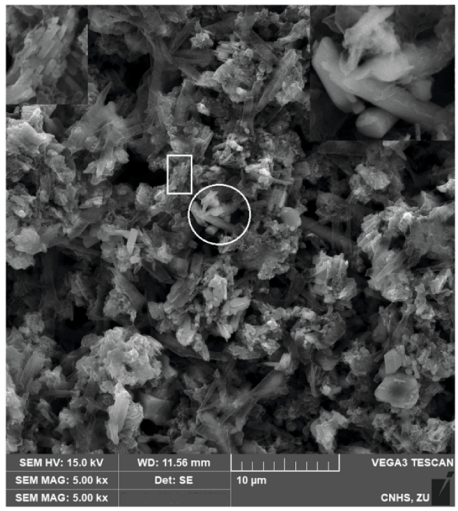

Figure 2: SEM micrograph of the as-synthesized $Mg_2B_2O_5$-Fe_3BO_6 composites. High magnification inset on the upper right and left are the portions tagged in white circle and rectangle.

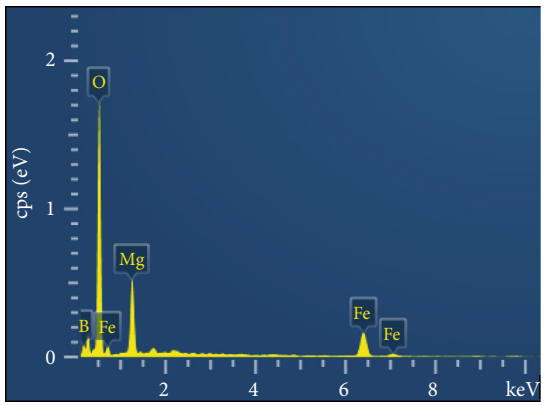

Element	Weight (%)	Atomic (%)
O	53.15	50.85
Mg	7.57	4.76
Fe	9.83	2.69
B	29.45	41.70
Total	100	100

Figure 3: EDX spectrum showing peaks for different compositions of $Mg_2B_2O_5$-Fe_3BO_6 composites. The table shows the weight and atomic percent of the elements in the synthesized composites.

the upper left-hand corner of the micrograph. The inset shows that the agglomerated structures are small crystals aligned in a particular pattern. It gives a clue that all of the composites start the growth in an aligned format. The growth continues until the crystal is sufficiently big enough due to the utilization of all growth species. The unavailability of the growth species causes irregular growth at higher temperatures. As a result, the crystals cannot maintain their align format and broke from their regular pattern. Thus, the synthesized $Mg_2B_2O_5$-Fe_3BO_6 composites are prepared in the shown irregular sizes and morphologies.

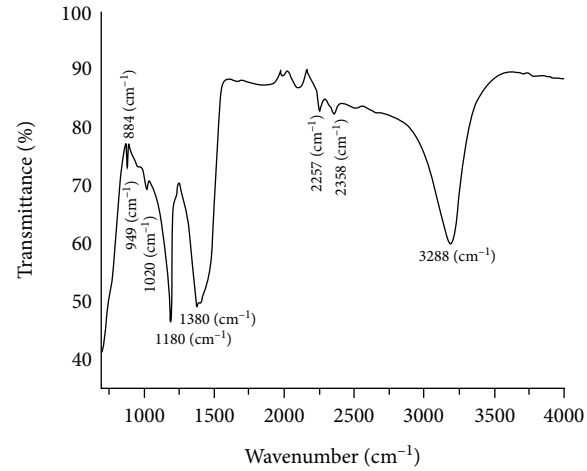

Figure 4: FTIR spectrum of the synthesized $Mg_2B_2O_5$-Fe_3BO_6 composites.

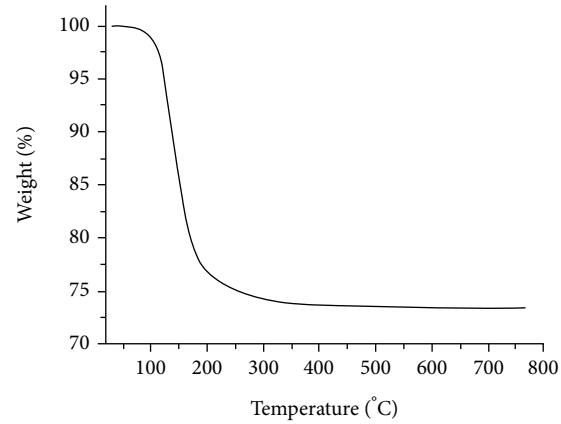

Figure 5: Thermogravimetric analysis curve of the as-synthesized $Mg_2B_2O_5$-Fe_3BO_6 composites.

Energy dispersive X-ray spectroscopy (EDX) of the synthesized $Mg_2B_2O_5$-Fe_3BO_6 composite sample has been performed to verify its elemental compositions. The acquired EDX spectrum is displayed in Figure 3. The displayed spectrum has various lower and higher intensity peaks. All the reported peaks are tagged with B, O, Fe, Mg, Fe, and Fe, respectively. These tags correspond to the boron, oxygen, magnesium, and iron compositions of the synthesized sample. Their weight and atomic percentages are also given in the table below the EDX spectrum. These percentages are in good agreement with the stoichiometric calculation of the synthesized composites.

The $Mg_2B_2O_5$-Fe_3BO_6 composites are further characterized by Fourier transform infrared spectroscopy (FTIR) to analyze their composition and bonding. The obtained FTIR spectrum is shown in Figure 4. The spectrum shows two peaks at 1020 (cm^{-1}) and 1180 (cm^{-1}). These two peaks are linked to the asymmetric stretching of the BO_4 group in $Mg_2B_2O_5$ [26, 27]. The bands at 1380 (cm^{-1}) are strong

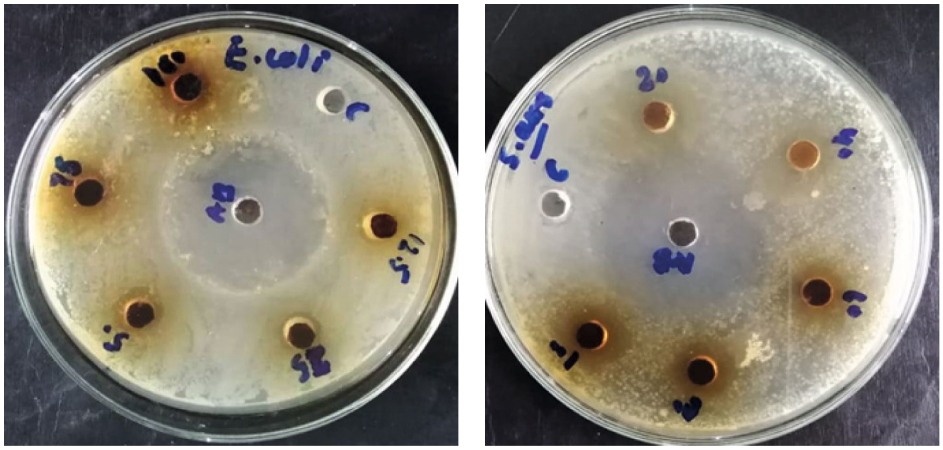

Figure 6: Zone of inhibition formed by different concentrations of $Mg_2B_2O_5$-Fe_3BO_6 composites against *S. aureus* (a) and *E. coli* (b).

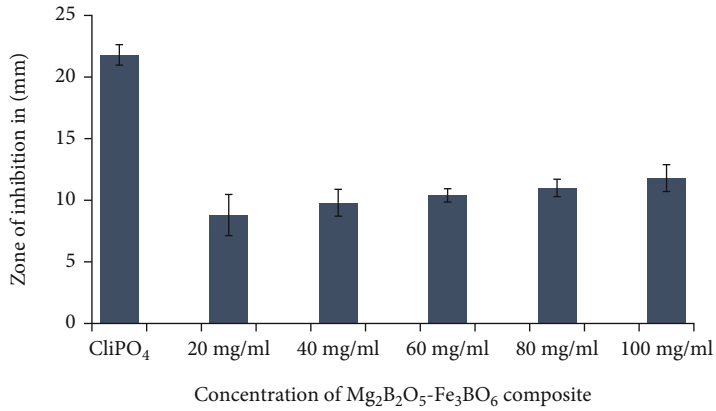

Figure 7: Bar chart of zone of inhibition formed by different concentrations of $Mg_2B_2O_5$-Fe_3BO_6 composites against *E. coli*.

absorption that stands for the asymmetric stretching of the BO_3 group. Likewise, the two small shoulder peaks found at 884 (cm^{-1}) and 949 (cm^{-1}) are weak absorptions due to BO_3 group vibration in Fe_3BO_6 [24]. Finally, the two very weak bands at 2257 (cm^{-1}) and 2358 (cm^{-1}) and one very strong peak at 3288 (cm^{-1}) are assigned to the stretching of O-H in hydrated borates [28, 29].

The thermal stability of the as-synthesized composites is checked in the thermogravimetric (TGA) analysis. The TGA curve of $Mg_2B_2O_5$-Fe_3BO_6 composites is depicted in Figure 5. The TGA curve shows two regions of weight loss as a consequence of increasing temperature. The first weight loss is observed in the temperature range of room temperature to 200°C. This steep weight loss is attributed to the evaporation of surface water from the surface of $Mg_2B_2O_5$-Fe_3BO_6 composites. The second weight loss is recorded from 200 to 300°C temperature zone. This weight loss indicates the dissociation of metal precursors used during the synthesis of borates composites. Overall, only 25 weight loss is observed up to 300°C, which verifies the thermal stability of magnesium borates and iron borate composite. Such thermal stability of both the borates is in good agreement with the literature [30, 31]. Previously, for the uncalcined powder of $Mg_2B_2O_5$, a 42% of weight loss was recorded [4], which is quite higher than the one calculated for our synthesized composites. Likewise, the total mass loss of the synthesized composites is far less than that observed for Fe_3BO_6 [7]. Thus, the as-synthesized $Mg_2B_2O_5$-Fe_3BO_6 composites are thermally more stable than the individual borates of iron and magnesium.

Materials have always been the main focus of researchers for different biomedical and biological applications such as antibacterial activities. In this regard, it is worth mentioning to apprise some of the excellent work done on Ag-NPs, ZnS nanoparticles, and tin-doped ZnO nanoparticles for antibacterial activities by different research groups [32–35].

Similarly, the current work is also an effort to observe the enhanced antibacterial activities of the synthesized $Mg_2B_2O_5$-Fe_3BO_6 composite.

The data obtained from the antibacterial analysis of the synthesized composite showed that $Mg_2B_2O_5$-Fe_3BO_6 inhibited the growth of both gram-positive and gram-negative bacteria as shown in Figures 6(a) and 6(b). The antibacterial

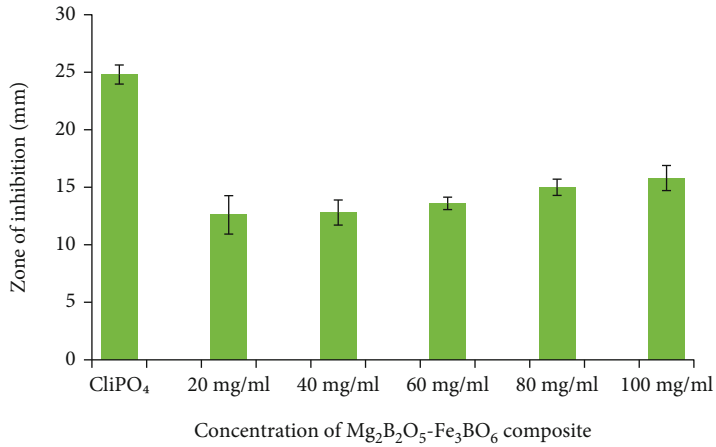

Figure 8: Bar chart of zone of inhibition formed by different concentrations of $Mg_2B_2O_5$-Fe_3BO_6 composites against *S. aureus*.

effect of $Mg_2B_2O_5$-Fe_3BO_6 was observed against both *S. aureus* and *E. coli* on all the tested doses and found to increase with an increase in $Mg_2B_2O_5$-Fe_3BO_6 composite concentration as shown in Figures 6(a) and 6(b). Against *E. coli*, the highest zone of inhibition diameter (11.8 mm) was recorded at 100 mg/ml concentration, whereas the smallest zone of inhibition diameter (8.8 mm) was observed at 20 mg/ml concentration. This can easily be seen and observed via a bar graph shown in Figure 7. Similarly, *S. aureus* showed the highest value of zone of inhibition (15.8 mm) at 100 mg/ml and the smallest zone of inhibition (12.6 mm) at 20 mg/ml (as shown in Figure 8).

The results showed that the inhibitory effect of composites was more pronounced against *S. aureus* than *E. coli* and found to form a greater zone of inhibition on all the tested doses. This is attributed to the differences in structure between gram-positive and gram-negative bacteria. The gram-positive bacteria have a thick cell wall, whereas gram-negative bacteria usually have a thin cell wall surrounded by an extra membrane.

4. Conclusions

Borates have excellent properties for different biological and biomedical applications including the antibacterial activity. $Mg_2B_2O_5$ and Fe_3BO_6 are the two well-known magnesium and iron borates synthesized and tested for its potential applications. In view of the excellent properties of the individual borates, composites of $Mg_2B_2O_5$ and Fe_3BO_6 were synthesized via a simple and easy to follow technique. The synthesized material composites of $Mg_2B_2O_5$ and Fe_3BO_6 were found to have far better thermal stability than their primary compounds. The data obtained from the antibacterial study showed that the as-synthesized composites of $Mg_2B_2O_5$-Fe_3BO_6 inhibited the growth of both gram-positive and gram-negative bacteria. The inhibitory effect of composites was more pronounced against *S. aureus* as compared to *E. coli* and form a greater zone of inhibition on all the tested doses. This work also revealed a potential role of boron-based composites in the inhibition of pathogenic bacteria and can therefore be used to control microbial infections.

Data Availability

All the data is available within the manuscript.

Conflicts of Interest

The authors declare no conflict of interest.

Acknowledgments

The authors extend their appreciation to the Higher Education Commission of Pakistan (HEC) for providing funds for our research work under the National Research Program for Universities (NRPU) project No. 10928. The authors gratefully acknowledge the Deanship of Scientific Research at King Khalid University for funding this work through General Research Project under grant number G.R.P/67/43.

References

[1] G. Wang, Q. Xue, X. She, and J. Wang, "Carbothermal reduction of boron-bearing iron concentrate and melting separation of the reduced pellet," *ISIJ International*, vol. 55, no. 4, pp. 751–757, 2015.

[2] E. Salama and H. Soliman, "Thermoluminescence glow curve deconvolution and trapping parameters determination of dysprosium doped magnesium borate glass," *Radiation Physics and Chemistry*, vol. 148, pp. 95–99, 2018.

[3] D. Ağaoğullari, Ö. Balci, H. Gökçe, İ. Duman, and M. L. Öveçoğlu, "Synthesis of magnesium borates by mechanically activated annealing," *Metallurgical and Materials Transactions A*, vol. 43, no. 7, pp. 2520–2533, 2012.

[4] A. Qasrawi, T. Kayed, A. Mergen, and M. Gürü, "Synthesis and characterization of $Mg_2B_2O_5$," *Materials Research Bulletin*, vol. 40, no. 4, pp. 583–589, 2005.

[5] S. Li, X. Fang, J. Leng, H. Shen, Y. Fan, and D. Xu, "A new route for the synthesis of $Mg_2B_2O_5$ nanorods by mechano-

chemical and sintering process," *Materials Letters*, vol. 64, no. 2, pp. 151–153, 2010.

[6] R. Diehl and G. Brandt, "Refinement of the crystal structure of Fe3BO6," *Chemistry*, vol. 31, no. 6, pp. 1662–1665, 1975.

[7] S. Ram, K. Kumari, and R. K. Kotnala, "Synthesis of norbergite Fe_3BO_6 of single crystallites from a borate glass," *Transactions of the Indian Ceramic Society*, vol. 69, no. 3, pp. 165–170, 2010.

[8] J. D. Lloyd, *Borates and their biological applications*, IRG Secretariat, Stockholm Sweden, 1998.

[9] T. Abdulrehman, S. Qadri, S. Skariah et al., "Boron doped silver-copper alloy nanoparticle targeting intracellular S. aureus in bone cells," *PLoS One*, vol. 15, no. 4, article e0231276, 2020.

[10] Y. Li, Z. Fan, J. G. Lu, and R. P. Chang, "Synthesis of magnesium borate ($Mg_2B_2O_5$) nanowires by chemical vapor deposition method," *Chemistry of Materials*, vol. 16, no. 13, pp. 2512–2514, 2004.

[11] B. Xu, T. Li, Y. Zhang, Z. Zhang, X. Liu, and J. Zhao, "New synthetic route and characterization of magnesium borate nanorods," *Crystal Growth and Design*, vol. 8, no. 4, pp. 1218–1222, 2008.

[12] X. Tao and X. Li, "Catalyst-free synthesis, structural, and mechanical characterization of twinned $Mg_2B_2O_5$ nanowires," *Nano Letters*, vol. 8, no. 2, pp. 505–510, 2008.

[13] K. Kumari, S. Ram, and R. Kotnala, "Effect of temperature on magnetic and impedance properties of Fe_3BO_6 of nanotubular structure with a bonded B_2O_3 surface layer," *Journal of Applied Physics*, vol. 123, no. 9, article 094101, 2018.

[14] Y. Liu, S. Peng, Y. Ding et al., "Synthesis and characterization of ferroferriborate (Fe_3BO_5) nanorods," *Advanced Functional Materials*, vol. 19, no. 19, pp. 3146–3150, 2009.

[15] K. Kumari, S. Ram, and R. Kotnala, "Self-controlled growth of Fe_3BO_6 crystallites in shape of nanorods from iron-borate glass of small templates," *Materials Chemistry and Physics*, vol. 129, no. 3, pp. 1020–1026, 2011.

[16] H. Qi and Q. Chen, "Preparation of plywood-like Fe_3BO_5 nanorods by a facile hydrothermal method at low temperature," *Chemistry Letters*, vol. 37, no. 7, pp. 752-753, 2008.

[17] P. Ahmad, M. U. Khandaker, Z. R. Khan, and Y. M. Amin, "Synthesis of boron nitride nanotubes via chemical vapour deposition: a comprehensive review," *RSC Advances*, vol. 5, no. 44, pp. 35116–35137, 2015.

[18] C. Valgas, S. M. Souza, E. F. Smânia, and A. Smânia Jr., "Screening methods to determine antibacterial activity of natural products," *Brazilian Journal of Microbiology*, vol. 38, no. 2, pp. 369–380, 2007.

[19] P. Ahmad, M. U. Khandaker, and Y. M. Amin, "Synthesis of highly crystalline multilayers structures of ^{10}BNNTs as a potential neutron sensing element," *Ceramics International*, vol. 41, no. 3, pp. 4544–4548, 2015.

[20] P. Ahmad, M. U. Khandaker, Y. M. Amin et al., "Catalytic growth of vertically aligned neutron sensitive 10Boron nitride nanotubes," *Journal of Nanoparticle Research*, vol. 18, no. 1, p. 25, 2016.

[21] C. Zhi, Y. Bando, C. Tan, and D. Golberg, "Effective precursor for high yield synthesis of pure BN nanotubes," *Solid State Communications*, vol. 135, no. 1-2, pp. 67–70, 2005.

[22] N. Horzum, *Synthesis and Characterization of MgB 2 Superconducting Wires*, Doctoral dissertation, Izmir Institute of Technology, Turkey, 2008.

[23] C. H. Lee, J. S. Wang, V. K. Kayatsha, J. Y. Huang, and Y. K. Yap, "Effective growth of boron nitride nanotubes by thermal chemical vapor deposition," *Nanotechnology*, vol. 19, no. 45, p. 455605, 2008.

[24] K. Kumari, "Phase analysis, FTIR/Raman, and optical properties of Fe_3BO_6 nanocrystallites prepared by glass route at moderate temperature in ambient air," *Journal of Molecular Structure*, vol. 1173, pp. 417–421, 2018.

[25] X. Zhang, G. Li, J. You et al., "Extraction of boron from ludwigite ore: mechanism of soda-ash roasting of lizardite and szaibelyite," *Minerals*, vol. 9, no. 9, p. 533, 2019.

[26] S. Marincea, "Ludwigite from the type locality, Ocna de Fier, Romania; new data and review," *The Canadian Mineralogist*, vol. 37, pp. 1343–1362, 1999.

[27] M. Yildirim, A. S. Kipcak, and E. M. Derun, "Sonochemical-assisted magnesium borate synthesis from different boron sources," *Polish Journal of Chemical Technology*, vol. 19, pp. 81–88, 2017.

[28] L. Jun, X. Shuping, and G. Shiyang, "FT-IR and Raman spectroscopic study of hydrated borates," *Spectrochimica Acta Part A: Molecular and Biomolecular Spectroscopy*, vol. 51, no. 4, pp. 519–532, 1995.

[29] W. Zhu, Q. Zhang, L. Xiang, and S. Zhu, "Green co-precipitation byproduct-assisted thermal conversion route to submicron $Mg_2B_2O_5$ whiskers," *CrystEngComm*, vol. 13, no. 5, pp. 1654–1663, 2011.

[30] B. Tran, K. Tieu, S. Wan et al., "Understanding the tribological impacts of alkali element on lubrication of binary borate melt," *RSC Advances*, vol. 8, no. 51, pp. 28847–28860, 2018.

[31] M. Bagherabadi, R. Naghizadeh, H. Rezaie, and M. Fallah Vostakola, "Synthesis of dehydrated magnesium borate powders and the effect on the properties of MgO-C refractories," *Journal of Ceramic Processing Research*, vol. 19, pp. 218–223, 2018.

[32] S. Kumar, T. W. Kang, S. J. Lee et al., "Correlation of antibacterial and time resolved photoluminescence studies using bio-reduced silver nanoparticles conjugated with fluorescent quantum dots as a biomarker," *Journal of Materials Science: Materials in Electronics*, vol. 30, no. 7, pp. 6977–6983, 2019.

[33] S. Kumar, S. Taneja, S. Banyal et al., "Bio-synthesised silver nanoparticle-conjugated l-cysteine ceiled Mn: ZnS quantum dots for eco-friendly biosensor and antimicrobial applications," *Journal of Electronic Materials*, vol. 50, no. 7, pp. 3986–3995, 2021.

[34] S. Kumar, A. Jain, S. Panwar et al., "Effect of silica on the ZnS nanoparticles for stable and sustainable antibacterial application," *International Journal of Applied Ceramic Technology*, vol. 16, no. 2, pp. 531–540, 2019.

[35] S. Kumar, H. Bhatti, K. Singh et al., "Effect of glutathione capping on the antibacterial activity of tin doped ZnO nanoparticles," *Physica Scripta*, vol. 96, no. 12, article 125807, 2021.